Qualification of a Multi-Channel Infrared Laser Absorption Spectrometer for Monitoring CO, HCl, HCN, HF, and CO_2 Aboard Manned Spacecraft

Ryan M. Briggs,[1] Clifford Frez,[2] and Siamak Forouhar[3]
Jet Propulsion Laboratory, California Institute of Technology, Pasadena, CA 91109, USA

Randy D. May[4]
Port City Instruments, Henderson, NV 89014, USA

Marit E. Meyer[5] and Michael J. Kulis[6]
NASA Glenn Research Center, Cleveland, OH 44135, USA

Gordon M. Berger[7]
National Center for Space Exploration Research, Cleveland, OH 44135, USA

Monitoring of specific combustion products can provide early-warning detection of accidental fires aboard manned spacecraft and also identify the source and severity of combustion events. Furthermore, quantitative *in situ* measurements are important for gauging levels of exposure to hazardous gases, particularly on long-duration missions where analysis of returned samples becomes impractical. Absorption spectroscopy using tunable laser sources in the 2 to 5 µm wavelength range enables accurate, unambiguous detection of CO, HCl, HCN, HF, and CO_2, which are produced in varying amounts through the heating of electrical components and packaging materials commonly used aboard spacecraft. Here, we report on calibration and testing of a five-channel laser absorption spectrometer designed to accurately monitor ambient gas-phase concentrations of these five compounds, with low-level detection limits based on the Spacecraft Maximum Allowable Concentrations. The instrument employs a two-pass absorption cell with a total optical pathlength of 50 cm and a dedicated infrared semiconductor laser source for each target gas. We present results from testing the five-channel sensor in the presence of trace concentrations of the target compounds that were introduced using both gas sources and oxidative pyrolysis (non-flaming combustion) of solid material mixtures.

Nomenclature

EC	=	electrochemical (sensor)
TLAS	=	tunable laser absorption spectrometer
2f	=	second harmonic (detection)
FPGA	=	field-programmable gate array
QC	=	quantum cascade (laser)

[1] Microdevices Engineer, JPL Microdevices Laboratory, Mail Stop 302-222.
[2] Microdevices Engineer, JPL Microdevices Laboratory, Mail Stop 302-205E.
[3] Group Leader, Advanced Microfabrication and Optoelectronics, JPL Microdevices Laboratory, Mail Stop 302-227.
[4] President, Port City Instruments, LLC.
[5] Research Engineer, Combustion and Reacting Systems Branch, Mail Stop 77-55.
[6] Research Engineer, Combustion and Reacting Systems Branch, Mail Stop 110-3.
[7] Research Engineer, Combustion and Reacting Systems Branch, Mail Stop 110-3.

IC	=	interband cascade (laser)
CW	=	continuous wave
DFB	=	distributed feedback
DC	=	direct current
TEC	=	thermoelectric cooler
MCT	=	mercury cadmium telluride (detector)
InAs	=	indium arsenide (detector)
InGaAs	=	indium gallium arsenide (detector)
CO	=	carbon monoxide
CO_2	=	carbon dioxide
HCl	=	hydrogen chloride
HCN	=	hydrogen cyanide
HF	=	hydrogen fluoride
PVC	=	polyvinyl chloride
PTFE	=	polytetrafluoroethylene
ppmv	=	part per million by volume
SLPM	=	standard liters per minute
FTIR	=	Fourier transform infrared (spectrometer)
SMAC	=	Spacecraft Maximum Allowable Concentration
GASP	=	Gases and Aerosols from Smoldering Polymers (Laboratory)

I. Introduction

As part of ongoing efforts to develop accurate and reliable manned spacecraft safety systems, NASA has continued to support the evaluation of instruments capable of monitoring key gases related to accidental combustion events. Continuous, high-rate measurements of the abundance of specific combustion products can assist in identifying fires caused by equipment malfunctions and provide valuable safety information for post-fire cleanup.[1-3] Monitoring systems currently employed on the International Space Station rely on electrochemical (EC) sensors (Industrial Scientific CSA-CP) as well as more complex gas chromatography and mass spectrometry systems. In general, EC sensors provide portable detection with potentially high sensitivity; however, they require maintenance and re-calibration, particularly with varying ambient pressure, and can exhibit cross-sensitivity between gases. Mass spectrometry sensors enable extremely high accuracy with a high degree of gas specificity, but often require substantial infrastructure. In contrast, tunable laser absorption spectrometer (TLAS) sensors combine accuracy and gas specificity with the potential for portable, continuous, and maintenance-free operation over a wide range of ambient pressures.[4]

Here, we report on development and initial testing of a prototype five-channel TLAS sensor designed to continuously monitor ambient concentrations of CO, HCl, HCN, HF, and CO_2, with low-level detection limits based on the relevant Spacecraft Maximum Allowable Concentrations (SMACs).[5] The TLAS instrument employs five individual semiconductor lasers purpose-built to interrogate specific infrared absorption lines of each compound using modulation spectroscopy with second-harmonic (2f) detection.[6] An initial calibration for each gas was established assuming a linear relationship between volume concentration and the 2f absorption amplitude with ambient pressure and temperature corrections.[7] We present concentration measurements obtained using reference gases as well as measurements of the emissions generated by oxidative pyrolysis of various materials using the Gases and Aerosols from Smoldering Polymers (GASP) Laboratory at NASA Glenn Research Center. Based on the reference gas measurements, we established the deviation from the initial linear calibration over the relevant concentration ranges of each gas. These nonlinear corrections were then used to calibrate the pyrolysis measurements. Finally, where possible, the measured combustion product concentrations are compared with measurements from a reference EC sensor.

II. Instrument Design

Figure 1 shows the prototype five-channel TLAS instrument, which is an extension of a previous instrument design implemented for CO monitoring.[8] The five-channel instrument is based on an open-cell configuration that is intended to operate at the same pressure and temperature as the ambient environment. A single heat-sink assembly accepts five sets of dedicated lasers and detectors and sits opposite a mirror bank to create a 50-cm two-pass optical path. Emission from each laser is collimated with an integrated lens before traversing the sampling region. Other than the detectors for the two shortest-wavelength channels, each laser and detector includes an integrated

thermoelectric cooler (TEC) for temperature stabilization. Dedicated electronics are used to simultaneously control the temperature of each laser and detector. The ambient temperature and pressure are measured with additional sensors integrated into the sampling region.

The TLAS instrument determines gas concentration by current-tuning the emission wavelength of each laser across the target absorption line with a 200 ms scan period. Five custom FPGA boards are used to supply current to the lasers and record the corresponding detector response. During each scan, a linear current ramp is applied to each laser with an additional small-amplitude sinusoidal current modulation at a frequency near 31.4 kHz, with a small frequency offset on each channel to avoid crosstalk. Using the FPGAs, the detector signals are demodulated at twice the modulation frequency to extract the second-harmonic (2f) response.[6,7] The quasi-DC response is also recorded after passing the signal through a low-pass filter. An integrated data acquisition board collects the 2f and DC spectra from each channel, along with the on-board pressure and temperature sensor readings, and streams the data to a single USB interface.

To achieve accurate low-level sensitivity with relatively short optical interaction length and minimal interference from other gases, we targeted the mid-infrared absorption lines listed in Table 1. A detailed description of absorption line selection has been presented previously.[9] Based on the performance of instruments using the same 2f detection scheme, we estimate a minimum resolvable line-center absorption sensitivity of 10^{-4}. To reach the required low-level sensitivities for CO and HCl with an optical pathlength of 50 cm, we targeted fundamental absorption lines at mid-infrared wavelengths that are difficult to access with conventional type-I interband diode lasers. Consequently, these long-wavelength channels rely on quantum cascade (QC) and interband cascade (IC) laser technology, respectively, while the remaining laser channels use distributed-feedback (DFB) type-I GaSb-based diode lasers.[10,11] The QC laser is based on a low-power-consumption DFB design that enables CW operation with approximately 1 W of input power, including temperature stablization.[12] The IC laser is based on a novel laterally coupled DFB grating design, which enables stable single-mode emission over a broad range of operating current and temperature with total power consumption below 1 W.[13] All five laser sources were fabricated and packaged in TO-3 enclosures with integrated TECs and thermistors. Each source exhibits CW mode-hop-free current tuning at or above room temperature, which minimizes the TEC power required to thermally stabilize the lasers.

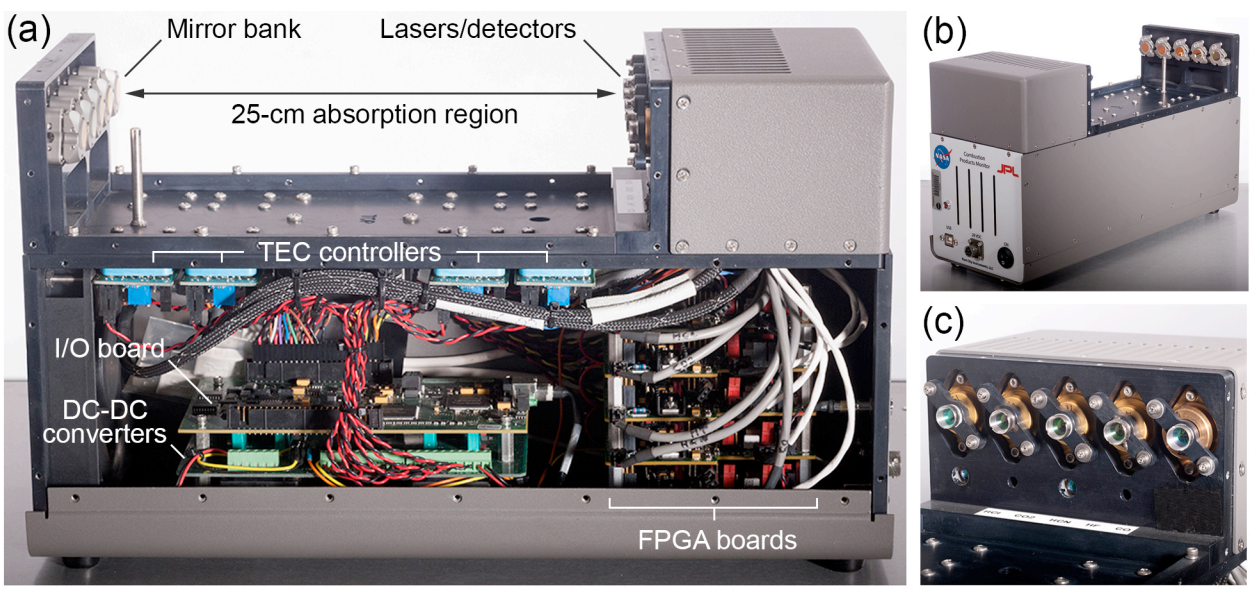

Figure 1. *(a) Layout of the five-channel TLAS instrument, shown with the protective covers removed from the sampling region and electronics compartment. Light from each laser source is reflected by a mirror back to a dedicated detector, resulting in a total optical pathlength of 50 cm. The sampling region can be fitted with either a perforated cover that protects the optical components while allowing ambient gases to pass through the optical path or a sealed cover that allows flow through input/output ports. (b) An alternate view of the instrument showing the front panel with power and USB communication interfaces. (c) A detailed view of the laser sources with collimation optics (top row) and the recessed detectors (bottom row).*

A TEC-stabilized MCT photodiode detector is used for the CO channel, while the HCl and HCN channels each employ a TEC-stabilized InAs photodiode. For the shorter-wavelength HF and CO_2 channels, we employed extended InGaAs photodiodes that require no thermal stabilization due to their high dynamic resistance and relatively temperature-insensitive responsivity. After conditioning the detector response with a preamp module on each FPGA board, the DC and 2f spectra were transmitted to a control computer for processing. For the testing reported here, five spectra from each channel were averaged prior to processing, resulting in an overall sampling rate of approximately 1 s. Fully assembled, the prototype TLAS instrument is 38 cm long, 23 cm tall, and 15 cm wide, with a total mass of 5 kg. The instrument consumes an average of 20 W while operating near room temperature with 28 V DC input. Future planned implementations of the sensor architecture will employ a single integrated FPGA board and a custom integrated temperature controller board in order to significantly reduce instrument volume, mass, and power consumption.

The TLAS instrument was initially calibrated by flowing a diluted mixture of the five target gases through a sealed flow cell placed in the optical path of each laser. For low concentrations, the peak-to-peak amplitude of the 2f absorption feature can be reliably used to quantitatively determine the concentration of each gas. At higher concentrations, where Beer's law effects become significant, a nonlinear calibration of the 2f amplitude was established based on the reference gas measurements described in the following section.

Table 1. *Spacecraft Maximum Allowable Concentrations for each target gas for various periods of exposure. Also listed are the target measurement range, absorption wavelength, relative on-resonance absorption, and selected laser technology for each gas detected by the five-channel TLAS instrument.*

Gas	Spacecraft Maximum Allowable Concentrations[5] (ppmv)	Target performance range (ppmv)	Target laser wavelength (nm)	Relative line-center absorption at lowest detection level	Laser technology
CO	1 h: 425 24 h: 100 7 d: 55 30+ d: 15	1 – 1000	4764.0	0.0020	Quantum cascade (QC) distributed-feedback (DFB) laser
HCl	1 h: 8 24 h: 4 7 d: 1 30+ d: 1	0.5 - 50	3572.8	0.0011	Interband cascade (IC) DFB laser
HCN	1 h: 5 24 h: 2.5 7d: 1 30+ d: 1	0.5 - 50	3001.5	0.0006	Laterally coupled DFB GaSb-based diode laser
HF	1 h: 5 24 h: 2 7d: 1 30+ d: 1	0.5 - 50	2395.8	0.0027	Laterally coupled DFB GaSb-based diode laser
CO_2	1 h: 20 000 24 h: 13 000 7 d: 7000 30+ d: 7000	300 – 30 000	2055.5	0.0006	Laterally coupled DFB GaSb-based diode laser

III. Testing Configuration and Instrument Calibration

The Gases and Aerosols from Smoldering Polymers (GASP) Facility was established at NASA Glenn Research Center to perform experiments related to spacecraft fire safety and post-fire environments. Figure 2 shows the configuration of the furnace, smoke chamber, and standard measurement instruments. For the tests reported here, *in situ* EC sensors were used for reference measurements, rather than the Fourier transform infrared (FTIR) spectrometer. Aerosol and particulate data collected during pyrolysis testing will be reported elsewhere. Safety considerations dictate that all aerosol and gas instruments – as well as all mechanical connections of tubing that

would contain smoke or corrosive gases – must be enclosed and vented continually to avoid toxic exposure to operators. One polycarbonate enclosure covers the smoke chamber and a separate larger cover on an optical table contains the furnace and other equipment. Access doors in the large enclosure allow samples to be loaded into the furnace as well as instrument adjustments between experiments.

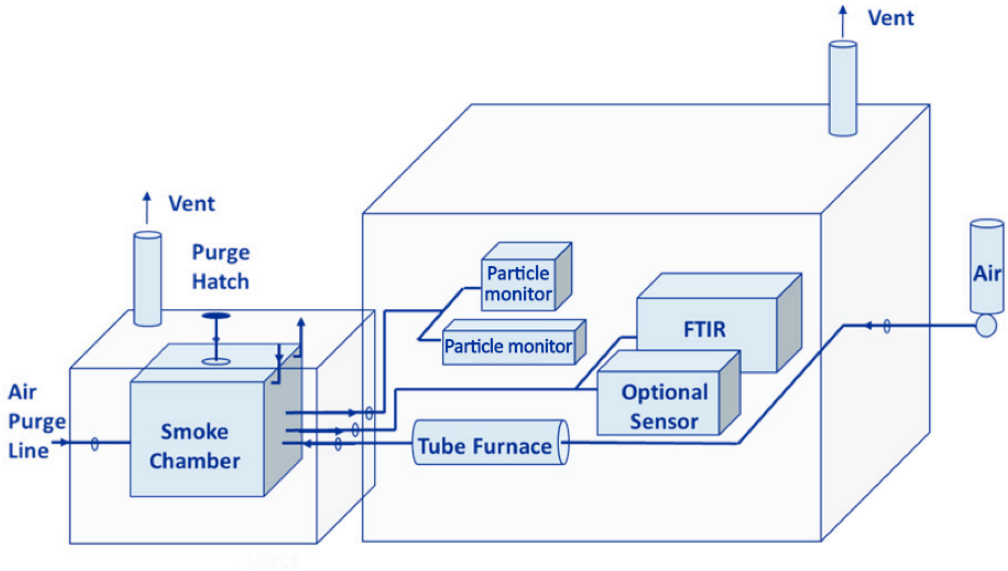

Figure 2. *GASP Facility diagram showing the furnace and standard instruments in the large enclosure, where the five-channel TLAS instrument was calibrated using reference gases. Combustion tests were conducted in the smoke chamber housed in the second enclosure on the left.*

For pyrolysis testing, the GASP Facility smoke chamber is vented by a purge hatch (without opening the enclosure), which directs the smoke through the vent as HEPA-filtered air is flushed through the chamber. Virtually particle-free air is obtained as the baseline for smoke tests (typically less than 20 #/cm^3). Another HEPA filter capsule is open at all times to allow gas to escape and prevent any potential over-pressurization of the smoke chamber. A Lindberg/Blue M tube furnace (HTF55322A) is used to heat samples and generate the oxidative pyrolysis products of interest for spacecraft fire safety (as opposed to flaming combustion products). The furnace has been thermally characterized to determine the optimal heating zone for fuel samples, and this temperature is logged throughout the duration of each test with a thermocouple mounted at the fuel sample location. During heating, filtered air flows through the furnace at 4.4 SLPM to flush the decomposition products into the 326-L smoke chamber. The smoke chamber includes passthroughs for the furnace tube (smoke/gas source) and tubing directed to aerosol dilution equipment and instruments, as well as data and power cables for instruments inside the smoke chamber. A small fan placed in the corner of the smoke chamber prevents stratification of smoke and gases. For the tests reported here, reference EC sensors were placed inside the enclosure along with the five-channel TLAS instrument. Data from the aerosol/particulate monitors shown in Fig. 2 will be reported elsewhere.

A vented gas cabinet houses bottles for reference gas testing in the GASP Facility. Stainless steel 0.25-in tubing delivers gases or filtered air by way of calibrated flow controllers to the large enclosure in Fig. 2. To minimize any safety issues, the ventilated cabinet containing the gas cylinders and all of the pressure and flow regulation instrumentation is connected to the ventilated testing area by a single run of stainless steel tubing approximately 20 ft long. The flow of the calibration gas and air diluent is regulated by thermal-based mass flow controllers (MKS Instruments). The system is set up to allow purging of the gas lines following each gas test. The pairing of mass flow controllers for the calibration tests allows for dilution from 1 to 100% of the full bottle concentration to test the high and low limits of sensing devices.

Using appropriate reference gases, quadratic calibration functions were established for CO, HCN, HCl, and CO_2 over the relevant concentration ranges for the TLAS instrument, as shown in Fig. 3. A sealed cover with gas ports was fitted over the absorption region of the TLAS instrument, enabling gas flow through the path of all the lasers simultaneously with minimal flow volume. The measured volume concentrations shown in Fig. 3 are based on the initial linear calibration with respect to 2f amplitude for each gas. We note that the linear calibrations are generally

accurate at low levels, with a few caveats. For HCN, noise due to optical fringes in the 2f spectrum prevented reliable concentration measurements below approximately 2 ppmv. For HCl, deviation from the initial calibration was observed for even modest levels, which is indicative of a significant dependence of the volatile HCl concentration on the flow channel configuration. In particular, compared with more inert species such as CO and CO_2, the measured HCl concentration was found to saturate slowly for a fixed HCl flow rate, suggesting strong interaction with the surfaces in the TLAS instrument and gas lines. Also, extensive purging with filtered air was required to remove all measurable amounts of HCl from the absorption region of the TLAS instrument. The HCl calibration shown in Fig. 3(c) was obtained by flowing the diluted reference gas at sequentially increasing concentrations through a fully purged system, while allowing the measured concentration to saturate at each level.

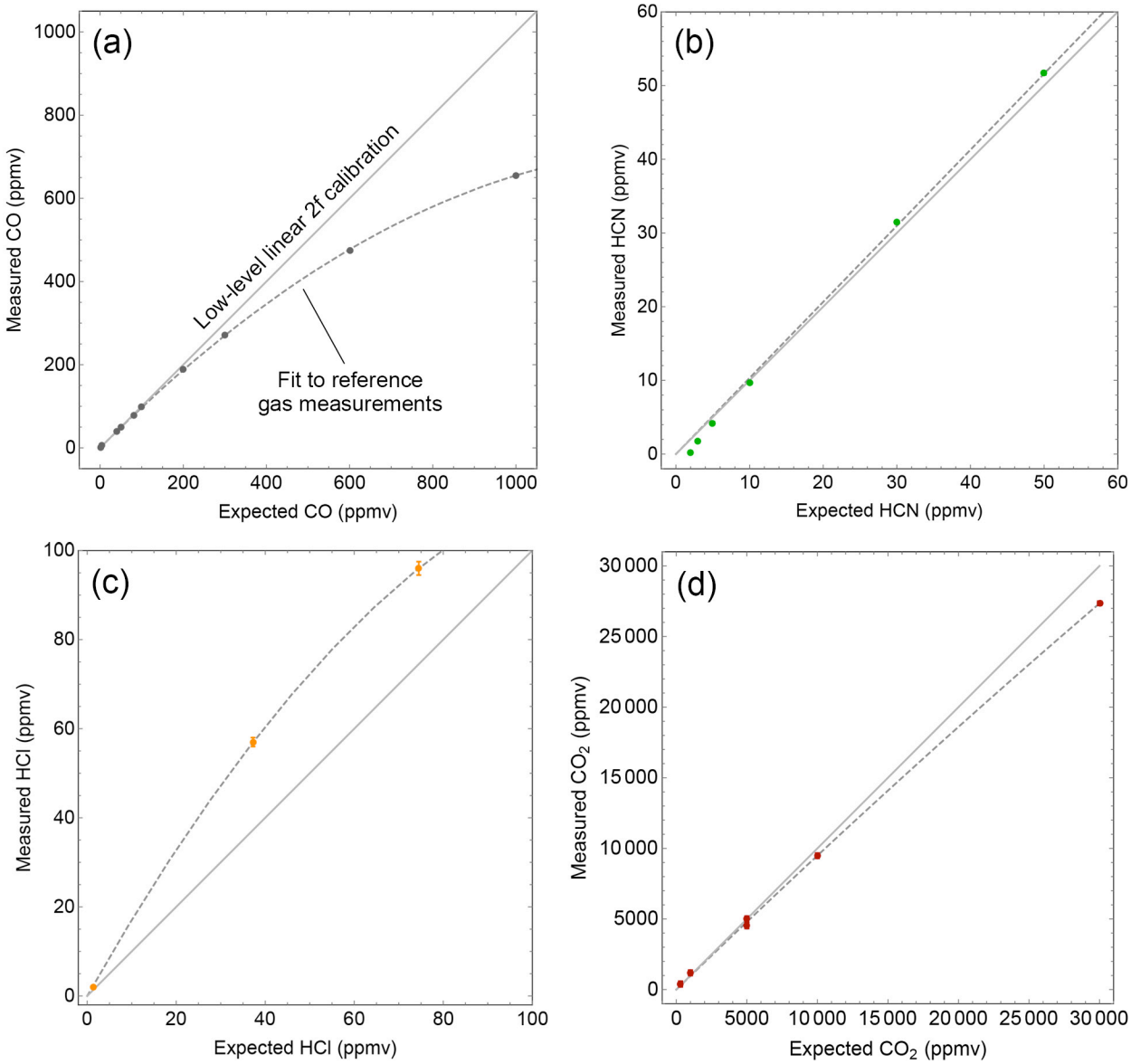

Figure 3. *Calibration of volume concentrations measured with the TLAS instrument for (a) CO, (b) HCN, (c) HCl, and (d) CO_2 collected at standard atmospheric temperature and pressure. Each data point corresponds to a measured concentration for a known dilution of the target compounds delivered from a reference gas cylinder. The dashed lines represent quadratic fits to the measured concentrations, which were used to calibrate the combustion product measurements presented in Section IV.*

Finally, we note that obtaining reliable HF concentration measurements with reference gas flows proved to be exceedingly challenging. When flowing HF gas dilutions directly through both the TLAS instrument and reference

EC sensors, the measured HF concentration saturated at a small fraction of the expected concentration. Ultimately, a linear calibration was established by placing a sealed static copper absorption cell with sapphire windows (Wavelength References) in the optical path of the TLAS instrument. The static cell was verified to contain a stable HF concentration in dry N_2 with absorption equivalent to 50 ppmv over an optical pathlength of 50 cm. Consequently, the HF concentration data reported for pyrolysis experiments in the following section should be interpreted as qualitatively accurate regarding the presence of HF as a combustion product; however, the HF channel was not as carefully calibrated over the full target concentration range as the four other TLAS channels.

IV. Combustion Product Testing

Using the GASP Facility smoke chamber, the TLAS instrument was exposed to emissions from the materials listed in Table 2. The sealed gas flow cover was replaced with a perforated cover to allow gases to freely pass through the optical path of the lasers. Fuel samples were placed in a 9-cm-long alumina boat (at room temperature) and weighed before and after heating. Starting at a furnace temperature of 200 °C with 4.4 SLPM of airflow through the tube furnace, the sample boat was inserted to the middle of the furnace tube. The furnace was heated to approximately 640 °C over a ramp time of 360 to 390 s. After allowing the sample to cool for several minutes, the smoke chamber was vented, as detailed in the previous section. Figure 4 shows the smoke chamber during a heating test as well as several fuel samples before and after oxidative pyrolysis.

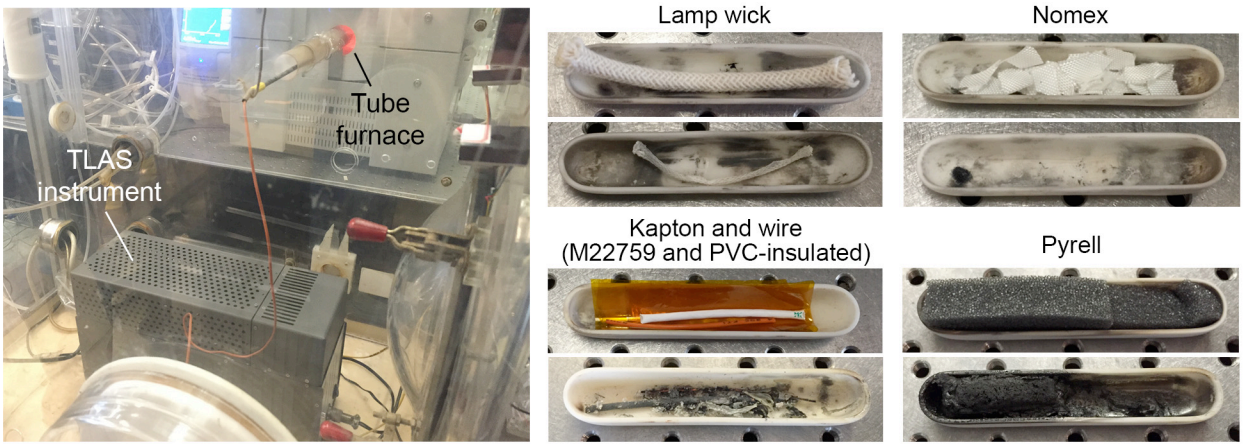

Figure 4. *Photograph of the smoke chamber during operation (left) and several fuel samples before and after heating to ~640 °C in the tube furnace. The five-channel TLAS instrument is shown inside the smoke chamber with a perforated cover over the optical path of the lasers.*

Table 2 lists the maximum observed concentration of each gas detected by the five-channel TLAS instrument for each fuel mixture. During heating, emissions levels often showed pronounced changes on the time scale of the sampling time (~1 s), as shown in Fig. 5, which we attribute to imperfect mixing in the smoke chamber during the initial stages of pyrolysis. Based on the amplitude of sample noise during cooling and venting, during which time concentration readings were observed to be less erratic, the precision for CO, HCN, HF, and HCl concentrations is better than 1 ppmv at total concentrations greater than 2 ppmv. We note that the overall uncertainty in concentration is impacted by uncertainty in the concentrations of the diluted reference gases used to calibrate the instrument as well as other unknown losses associated with the calibration measurements (including, for example, leaks in the sealed cover used to flow calibration gases through the absorption region of the TLAS instrument). Improved validation and control over calibration error will be implemented in future testing.

For all of the pyrolysis tests conducted here, the generated levels of CO_2 were relatively small compared with the full range of the TLAS instrument. Since the minimum detection limit of the CO_2 channel is comparable to standard ambient CO_2 levels, the CO_2 concentrations reported in Table 2 represent the observed average *increase* over the baseline level recorded by the TLAS instrument prior to heating the fuel samples. For the other four gases, the reported concentrations are taken to be absolute values, since ambient levels prior to heating are assumed to be below the corresponding minimum detection limits. Based on the standard deviation of sample-to-sample noise in the CO_2 concentration, we assign an additional uncertainty of 200 ppmv to the reported relative CO_2 levels.

Table 2 also includes measurements from a calibrated EC sensor (Dräger X-am 5600) with sensitivity to CO, HCN, and CO_2. For several samples that were expected to generate little or no HCN, there was evidence of cross

sensitivity of the EC sensor's HCN channel corresponding to the presence of HCl and HF. Based on fuel composition and comparisons with the TLAS measurements, we observed enhanced HCN readings with increasing HCl concentration and suppressed HCN readings with increasing HF concentration. There is insufficient data to conclude that the EC sensor was responding specifically to HCl and/or HF, since a variety of unmeasured compounds could have been present (such as Cl_2). Finally, we note that the CO_2 levels reported for the EC sensor are *absolute* concentrations, and the baseline CO_2 reading between tests was observed to be 300 to 400 ppmv, as expected for standard ambient conditions. Concentration measurements from the EC sensor are reported according to the display resolution for each gas: 1 ppmv for CO, 0.1 ppmv for HCN, and 100 ppmv for CO_2.

Table 2. *Summary of combustion testing for various materials heated to ~640 °C. Maximum gas concentrations are given based on measurements using the five-channel TLAS instrument and a reference EC sensor.*

Test	Material(s)	Component mass (g)	Total post-burn mass (g)	TLAS measured maximum concentration (ppmv) †					EC sensor maximum concentration (ppmv)		
				CO	HCN	HF	HCl	CO_2	CO	HCN	CO_2 ††
1	Kapton snips	0.505	0.243	585	13	<1	<1	600	525	11.4	1,000
2	Granulated PVC, 10 AWG M22759 wire, fibrous protein	0.100, 1.500, 0.250	1.367	132	12	35	75	400	124	27	700
3	Teflon (PTFE)*	0.503	~0	30	<1	110	19	600	28	~0	500
4	24-AWG wire (orange PVC insulation)	0.207 (~0.1 PVC)	0.121	16	<1	1	91	<300	16	4.3	600
5	Printed circuit board	1.481	1.130	182	<1	3	12	900	162	1.7	900
6	Electronic components**	0.598	0.378	95	<1	<1	<1	<300	86	1.8	700
7	Lamp wick	0.499	0.378	277	<1	<1	<1	<300	248	9.0	700
8	Nomex snips	0.253	0.001	281	3	<1	<1	1,000	260	2.0	1,100
9	Kapton bulk film, 10-AWG M22759 wire, 24-AWG wire (PVC)	0.250, 1.520, 0.208	1.463	419	<1	47	87	1,000	370	~0	1,500
10	Pyrell foam	0.500	0.056	164	8	<1	<1	600	158	9.8	500
11	Kapton bulk film (long burn)	0.503	0.011	854	12	<1	<1	1,300	725	2.0	1,600

* *To maximize HF yield, an inline water bubbler was used during this test to introduce humidity into the air flowing through the tube furnace. We speculate that the HCl reading is due to residual material from the previous test.*

***Component mixture included thin film resistors, a tantalum capacitor, an inductor, and a resin-encapsulated LED.*

† *Concentrations of CO, HCN, HF, and HCl are absolute values with uncertainty of 1 ppmv for levels greater than 2 ppmv (neglecting systematic error from calibration). The maximum CO_2 concentration reported is the average increase over the background level observed prior to heating. The uncertainty in relative CO_2 concentration is 200 ppmv based on the observed sampling noise.*

††*Concentrations of CO_2 reported for the EC sensor are absolute values as opposed to the relative values reported for the TLAS instrument.*

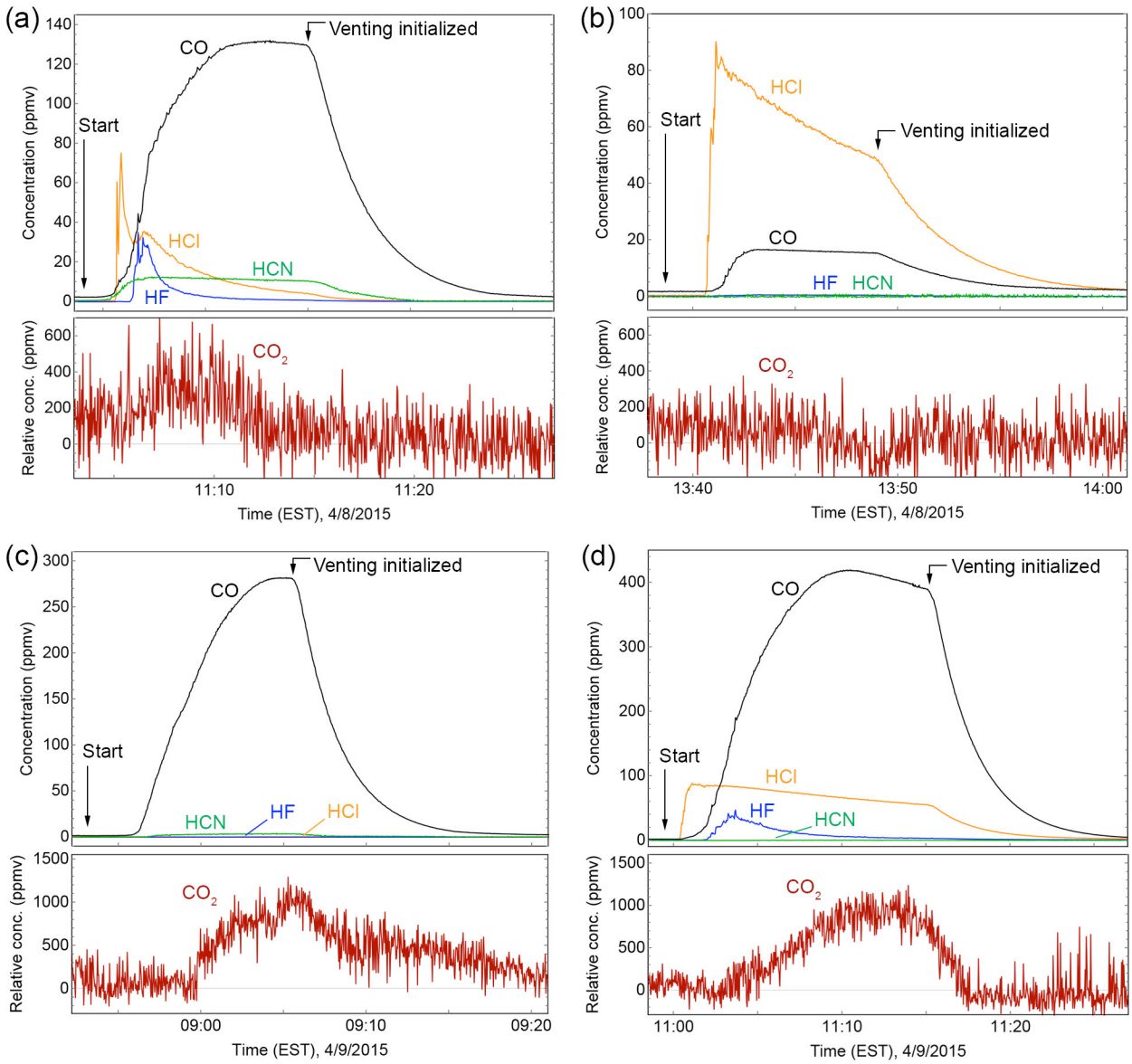

Figure 5. *Gas concentrations measured as a function of time with the five-channel TLAS instrument for the following fuels (described in Table 2): (a) a mixture of granulated PVC, M22759 insulated wire, and fibrous protein (test 2); (b) PVC-insulated wire (test 4); (c) Nomex (test 8); and (d) a mixture of Kapton, M22759 insulated wire, and PVC-insulated wire (test 9). The indicated concentrations of CO, HCN, HF, and HCl are absolute values, whereas the zero-level of the CO_2 concentration is the average reading prior to sample heating (assumed to be the ambient background level).*

Time-resolved TLAS measurements from four pyrolysis tests are shown in Fig. 5. Figure 5(a) shows levels of the target combustion products generated by heating a mixture of granulated PVC, 10-AWG M22759 insulated wire, and fibrous protein (a source of HCN). Figure 5(b) shows emissions from 25-AWG electrical wire with PVC insulation. Figure 5(c) shows emissions from Nomex pieces. Finally, the emissions shown in Fig. 5(d) correspond to a mixture of Kapton film, M22759 insulated wire, and wire with PVC insulation.

Comparing the quantitative concentration measurements obtained with the TLAS instrument and the reference EC sensor, we see clear agreement for measured CO concentration. In all tests, the maximum measured concentration of CO fell within 20% between the two sensors. For CO_2, there is qualitative agreement between the

two sensors for fuel samples that generated CO_2 at levels significantly above ambient concentrations (refer to tests 8, 9, and 11, for example, where both sensors read at or above 1000 ppmv). For the TLAS instrument, however, the combination of the relatively higher CO_2 detection limit and additional sample noise likely lead to quantitative inaccuracies, particularly below 1000 ppmv. Given that the CO_2 yield in all pyrolysis tests was significantly below the maximum target concentration of 30 000 ppmv, future TLAS instruments would benefit from higher CO_2 measurement accuracy at low concentrations (below 300 ppmv).

For HCN, we see agreement between the TLAS and EC sensors in pyrolysis tests where the TLAS instrument indicated no appreciable concentration of HF or HCl. In particular, heating of Kapton, Nomex, and Pyrell (tests 1, 8, and 10, respectively), produced HCN without the other corrosive gases, and the measured levels from the two sensors agree to within 2 ppmv. An exception is the final test with Kapton alone (test 11); however, a calibration error was suspected with the EC sensor due to questionable baseline readings immediately prior to the test. Also, the EC sensor measured HCN during oxidative pyrolysis of lamp wick (test 7), which is composed primarily of cellulose and would not be expected to produce significant amounts of HCN. We also observed elevated HCN readings on the EC sensor during pyrolysis tests that were expected to produce significant amounts of HCl without significant levels of the other corrosive gases (such as test 4, which used PVC-insulated wire). This implies positive cross-sensitivity with one or more compounds generated by chlorine-rich fuels, but more extensive testing is required to establish a definitive correlation with a specific compound. Additionally, in tests that produced significant amounts of HF without appreciable HCN (tests 3 and 9, in particular, which both used fuel samples containing PTFE), we observed below-zero HCN readings on the EC sensor, suggesting negative cross-sensitivity with one or more compounds generated by fluorine-rich fuels.

V. Conclusion

We have described testing of a five-channel laser spectrometer designed for continuous low-level monitoring of CO, HCl, HCN, HF, and CO_2 in manned spacecraft environments. The instrument was calibrated using gas standards at NASA Glenn Research Center and then challenged with pyrolysis tests using various materials relevant to spacecraft fire safety. The TLAS instrument employs a dedicated laser source to interrogate a specific absorption line of each target gas without interference from other species expected to be present in habitable environments. The lack of cross-sensitivity between the target gases was verified during calibration with individual reference gases, and, upon heating various fuel mixtures to generate unique combinations of emissions, we observed the presence or absence of the target gases independently.

Based on calibration measurements with CO and CO_2, we observed detection thresholds consistent with the target sensitivities listed in Table 1 and well below the 30-d SMACs. As mentioned above, however, future instruments should target even lower minimum detection levels for CO_2 in order to reliably account for ambient CO_2 levels in typical habitable atmospheres. Optical interference fringes in the TLAS sampling region prevented HCN detection below approximately 2 ppmv, which is above our target sensitivity of 0.5 ppmv but comparable to the 24-h SMAC of 2.5 ppmv. Finally, the inherent difficulties associated with delivering HF and HCl from gas sources impeded careful calibration of those channels; however, during pyrolysis testing, the TLAS sensor unambiguously detected the presence of HF and HCl with sampling noise below 1 ppmv and also showed a continuous change in the measured concentrations of those gases down to ambient levels (assumed to be well below 1 ppmv). This behavior suggests a detection threshold commensurate with out target of 0.5 ppmv for HF and HCl, but further studies should be conducted to verify accurate low-level detection of these gases.

The combustion product testing reported here is intended to be an initial demonstration of a laser-based instrument capable of specific detection of CO, HCl, HCN, HF, and CO_2 with sensitivities below the Spacecraft Maximum Allowable Concentrations. This initial testing provides a guide for future design improvements, including targeting a stronger CO_2 absorption line for below-ambient measurements and reducing reflections from collimation optics to avoid optical fringes affecting low-level HCN measurements. Looking ahead, while more rigorous calibration and testing is needed (particularly for HF and HCl), the laser absorption spectrometer architecture presented here has been shown to be an effective approach for real-time *in situ* multi-gas monitoring.

Acknowledgments

Part of this work was performed at the Jet Propulsion Laboratory (JPL), operated by the California Institute of Technology, under contract with the National Aeronautics and Space Administration. We thank P. D. Mudgett at NASA Johnson Space Center, M. L. Homer at JPL, and G. A. Ruff at NASA Glenn Research Center for testing support. We also gratefully acknowledge J. Joshi, N. Toomarian, D. J. Eisenman, and the NASA Life Support Systems Project under the Advanced Exploration Systems (AES) Program for critical support.

References

[1] Ruff, G. A., Greenberg, P. S., Mudgett, P. D., Hornung, S. D., Pilgrim, J. S., and Vakhtin, A. B., "Towards the Identification of Chemical Markers for Spacecraft Post-fire Cleanup," 41st International Conference on Environmental Systems, American Institute of Aeronautics and Astronautics (AIAA), Portland, Oregon, 17-21 July, 2011.

[2] Meyer, M. E., Mudgett, P. D., Hornung, S. D., McClure, M. B., Pilgrim, J. S., Bryg, V., Ruff, G. A., and Hunter, G., "Materials Combustion Testing and Combustion Product Sensor Evaluations in FY12," 43rd International Conference on Environmental Systems, American Institute of Aeronautics and Astronautics (AIAA), Vail, Colorado, 14-18 July, 2013.

[3] Kulis, M. J., Meyer, M. E., Mudgett, P. D., Berger, G. M., and Pilgrim, J. S., "Heating of Printed Circuit Board, Wire Insulation and Electronic Components for Fire Signature Sensor Evaluation," 44th International Conference on Environmental Systems, American Institute of Aeronautics and Astronautics (AIAA), Tucson, Arizona, 13-17 July, 2014.

[4] Kosterev, A., Wysocki, G., Bakhirkin, Y., So, S., Lewicki, R., Fraser, M., Tittel, F., and Curl, R. F., "Application of quantum cascade lasers to trace gas analysis," *Applied Physics B*, Vol. 90, No. 2, 2008, pp. 165-176.

[5] Committee on Spacecraft Exposure Guidelines, Committee on Toxicology, National Research Council, *Spacecraft Maximum Allowable Concentrations for Selected Airborne Contaminants*, Vol. 5, The National Academies Press, Washington, DC, 2008, pp. 125-142.

[6] May, R. D. and Webster, C. R., "Data processing and calibration for tunable diode laser harmonic absorption spectrometers," *Journal of Quantitative Spectroscopy and Radiative Transfer*, Vol. 49, No. 4,1993, pp. 335-347.

[7] Webster, C. R., May, R. D., Trimble, C. A., Chave, R. G., and Kendall, J., "Aircraft (ER-2) laser infrared absorption spectrometer (ALIAS) for *in-situ* stratospheric measurements of HCI, N_2O, CH_4, NO_2, and HNO_3," *Applied Optics*, Vol. 33, No. 3,1994, pp. 454-472.

[8] Briggs, R. M., Frez, C. , Forouhar, S., May, R. D., and Ruff, G. A., "Portable 4.6 µm Laser Absorption Spectrometer for Carbon Monoxide Monitoring and Fire Detection," 43rd International Conference on Environmental Systems, American Institute of Aeronautics and Astronautics (AIAA), Vail, Colorado, 14-18 July, 2013.

[9] Briggs, R. M., Frez, C., Borgentun, C. E., Bagheri, M., Forouhar, S., and May, R. D., "Five-Channel Infrared Laser Absorption Spectrometer for Combustion Product Monitoring Aboard Manned Spacecraft," 44th International Conference on Environmental Systems, American Institute of Aeronautics and Astronautics (AIAA), Tucson, Arizona, 13-17 July, 2014.

[10] Forouhar, S. Briggs, R. M., Frez, C., Franz, K. J., and Ksendzov, A., "High-power laterally coupled distributed-feedback GaSb-based diode lasers at 2 µm wavelength," *Applied Physics Letters*, Vol. 100, 2012, 031107.

[11] Briggs, R. M., Frez, C., Bagheri, M., Borgentun, C. E., Gupta, J. A., Witinski, M. F., Anderson, J. A., and Forouhar, S., "Single-mode 2.65 µm InGaAsSb/AlInGaAsSb laterally coupled distributed-feedback diode lasers for atmospheric gas detection," *Optics Express*, Vol. 21, 2013, pp. 1317-1323.

[12] Briggs, R. M., Frez, C., Borgentun, C. E., and Forouhar, S., "Regrowth-free single-mode quantum cascade lasers with power consumption below 1 W," *Applied Physics Letters*, Vol. 105, 2014, 141117.

[13] Borgentun, C. E., Frez, C., Briggs R. M., Fradet, M., and Forouhar, S., "Single-mode high-power interband cascade lasers for mid-infrared absorption spectroscopy," *Optics Express*, Vol. 23, 2013, pp. 2446-2450.